European Review for Medical and Pharmacological Sciences 2020; 24: 3538-3547

Mechanism of FGF7 gene silencing in regulating viability, apoptosis, invasion of retinoblastoma cell line HXO-Rb44 and angiogenesis

W.-J. CHEN[1], C.-X. SUN[2], W. LI[3]

[1]Department of Orthopedics Surgery, Tongji Hospital Affiliated with Tongji Medical College of Huazhong University of Science & Technology, Wuhan, Hubei Province, China
[2]Department of Ophthalmology, Yueyang Huashahengkang Hospital, Yueyang, Hunan Province, China
[3]Department of Ophthalmology, Union Hospital Affiliated with Tongji Medical College of Huazhong University of Science & Technology, Wuhan, Hubei Province, China

Abstract. – OBJECTIVE: To explore the mechanism of fibroblast growth factor 7 (FGF7) gene silencing in regulating viability, apoptosis, invasion of retinoblastoma (RB) cell line HXO-Rb44 and angiogenesis.

MATERIALS AND METHODS: Human normal retinal vascular endothelial cells ACBRI-181 was set as the normal group. The cultured RB cell lines HXO-Rb44 were divided into three groups: the blank group (without plasmid transfection), negative control group (transfection of FGF7 plasmid), and the si-FGF7 group (transfection of FGF7 siRNA plasmid). Quantitative Real Time-Polymerase Chain Reaction and Western blot were used to measure the mRNA and protein expression of B-cell lymphoma 2 (Bcl-2), Bcl-2-associated X protein (Bax), vascular endothelial growth factor (VEGF), basic fibroblast growth factor (bFGF), angiopoietin-2 (Ang-2), and proliferating cell nuclear antigen (PCNA) in each group. The 3-(4,5-dimethylthiazol-2-yl)-2,5-diphenyltetrazolium bromide (MTT) assay, transwell invasion assay, and flow cytometry were used, respectively, to assess cell viability, invasive capability, and cell apoptosis in each group.

RESULTS: The mRNA and protein expression of FGF7, Bcl-2, VEGF, bFGF, Ang-2, and PCNA were significantly decreased, and the mRNA and protein expression of Bax were significantly increased in the si-FGF7 group than in the blank group (all $p<0.05$). Compared with the blank group, the si-FGF7 group had significantly decreased cells invasive capability, cell viability at 48 h and 72 h and proliferation, and significantly increased apoptosis rate (all $p<0.05$).

CONCLUSIONS: FGF7 gene silencing can inhibit the viability and invasion of RB cells and the expression of angiogenesis-related factors and can promote RB apoptosis.

Key Words:
Gene silencing, Retinoblastoma, Apoptosis, Invasion.

Introduction

Retinoblastoma (RB) is a common primary intraocular malignant cancer in children that arises mainly in the embryonal nuclear layer of the retina. Retinoblastoma is often accompanied by strabismus and leukocoria in children[1]. Early diagnosis and treatment of RB is the key to improve eye retention rate. However, many children with RB in China are at the middle and advanced stage upon diagnosis and can only survive through enucleation of the eye[2]. Current treatments for RB mainly include local treatment modalities, such as enucleation, interventional therapy, cryotherapy and laser photocoagulation, chemotherapy, and gene therapy[3]. Gene therapy is a new approach to the treatment of tumors in recent years. It mainly uses genes as therapeutic targets to selectively kill tumor cells and promote their apoptosis[4]. Most tumors exhibit the inactivation of tumor suppressor genes and significant activation of proto-oncogenes[5,6]. Jia et al[7] confirmed that the inhibition of ABCG2 gene expression can significantly suppress the growth of RB. Angiogenesis plays an important role in the growth of RB. Therefore, the inhibition of neovascularization is a potentially effective approach for the treatment of RB[8]. Yang et al[9] confirmed by *in vitro* research that

Corresponding Author: Wan Li, MD; e-mail: liwan623@sina.com

the increase of the expression of pigment epithelium-derived factor (PEDF) gene can effectively reduce the angiogenesis of RB and promote the apoptosis of RB cells. Fibroblast growth factor 7 (FGF7), also known as keratinocyte growth factor (KGF) for its effect of promoting the mitosis of keratinocytes, was first isolated and purified by Rubin et al[10] from the supernatant of human embryonic lung fibroblasts. Since KGF needs to bind to its receptor, which is mainly distributed in epithelial cells, to perform its function, KGF is also considered to mainly act on epithelial cells[11]. Husseman et al[12] also confirmed that FGF7 can promote the proliferation of vascular endothelial cells and accelerate neovascularization. Current research on FGF7 demonstrates that it plays a catalytic role in the progression of a variety of tumors. Huang et al[13] found that FGF7 and its receptor FGFR2 were significantly increased in gastric cancer tissues, and the *in vitro* studies found that the overexpression of FGF7 could promote the migration and invasion of gastric cancer cells. Fan et al[14] found that FGF7 overexpression is an independent risk factor for bladder cancer and urothelial carcinoma. In addition, Shang et al[15] observed that miR-381-3p can specifically inhibit the expression of FGF7 gene and, therefore, suppress the proliferation of cervical cancer cells. However, the association between the FGF7 gene and the pathogenesis of RB remains unclear. From the perspective of gene-targeted therapy, we studied the effect of FGF7 gene expression on the biological characteristics of RB cells and the tumor angiogenesis by silencing FGF7 gene using RNA interference technology, aiming at providing theoretical basis and experimental evidence for RB gene therapy targeting FGF7.

Materials and Methods

Cell Grouping and Transfection

RB cell line HXO-Rb44 and human normal retinal vascular endothelial cell line ACBRI-181 were purchased from the cell center of Xiangya School of Medicine, Central South University. The cell lines were cultured as adherent cells in Roswell Memorial Park Institute (RMPI-1640) medium (Thermo Fisher Scientific, Inc., Waltham, MA, USA) supplemented with 10% fetal bovine serum (FBS; Thermo Fisher Scientific, Inc., Waltham, MA, USA) at 37°C in a 5% CO_2 incubator. The cells were routinely passaged every 3 days and the cells in the log phase were used in all experiments. Human normal retinal vascular endothelial cells ACBRI-181 were set as the normal group. RB cell lines HXO-Rb44 were divided into three groups: the blank group (without plasmid transfection), negative control (NC) group (transfection of FGF7 plasmid), and the si-FGF7 group (transfection of FGF7 siRNA plasmid).

FGF7 siRNA (5'-CCCTGAGCGACACACAAGAAGTTAT-3') and negative control sequence (5'-CCCGCGACACAAACAGAAGTGTTAT-3') were designed by BLOCK-iT™ RNAi Designer and synthesized by The Beijing Genomics Institute (BGI, Beijing, China). These sequences were respectively constructed into the plasmid vector pcDNA3.1 with Hind III and XHo I restriction enzyme sites at 16°C overnight. The recombinant pcDNA3.1-FGF7 plasmids were added to DH5α for transformation. Antibiotic-resistant colonies were screened and identified by colony digestion PCR and amplified, and the plasmids were extracted and stored at -20°C.

The cells in each group were inoculated into a 24-well plate, with five replicate wells for each group. When the confluence reached 50%-60%, transfection was performed using Lipofectamine™ 2000 Transfection Reagent (Invitrogen, Carlsbad, CA, USA) according to its instructions. Liposomes and target RNA mixture were prepared in two separate sterile Eppendorf (EP; Hamburg, Germany) tubes. The liposomes were prepared by mixing 1 μl Lipofectamine 2000 with 100 μl serum-free medium and were kept at room temperature for 5 min. The target RNA mixture was prepared by mixing 20 pmol target RNA with 50 μl serum-free medium. The RNA mixture was then mixed with liposomes to allow the formation of RNA-liposome complex. The complex was then kept at room temperature for 20 min before being added to the cell cultures and incubated at 37°C in a 5% CO_2 incubator. After 6-8 h of incubation, these cells were grown in complete growth medium for 24-48 h before the performance of subsequent experiments. All plasmids were purchased from RiboBio Co., (Guangzhou, China).

mRNA Expression of Genes by Quantitative Real Time-Polymerase Chain Reaction (qRT-PCR)

Cells were collected 48 hours after transfection, and centrifuged at 2,000 r/min. The supernatants were discarded, followed by RNA extraction for cells in each group according to the instructions of TRIzol reagent (Thermo Fisher Scien-

tific, Inc., Waltham, MA, USA). The primers for FGF7, B-cell lymphoma 2 (Bcl-2), Bcl-2-associated X protein (Bax), vascular endothelial growth factor (VEGF), proliferating cell nuclear antigen (PCNA), and glyceraldehyde 3-phosphate dehydrogenase (GAPDH) were designed and synthesized by TaKaRa Bio Inc. (Dalian, China), as shown in Table I. Reverse transcription of RNA was performed using PrimeScript RT reagent kit (RR036A; TaKaRa Bio Inc., Dalian, China). The reverse transcription was carried out according to the manufacturer's instructions of the kit based on 10 μl reactions. Each reaction was incubated at 37°C for three times, each time 15 min, followed by inactivation of reverse transcriptase at 85°C for 5 min. The reaction solutions were then harvested to carry out quantitative fluorescence PCR according to the instructions of SYBR® Premix Ex Taq™ II Kit (RR820A; TaKaRa Bio Inc., Dalian, China). The 50-μl reaction consisted of 25 μl of SYBR® Premix Ex Taq™ II (2×), 16 μl of ddH2O, 4 μl of DNA template, 2 μl of upstream primers, 2 μl of downstream primers, and l μl of ROX Reference Dye (50×). ABI 7500 Real-Time PCR System (7500, Applied Biosystems, Waltham, MA, USA) was used to conduct real-time fluorescence quantitative PCR. The reaction conditions were set as follows: 40 cycles of initial denaturation at 95°C for 30 sec, denaturation at 95°C for 5 sec, and annealing and extension at 60°C for 30 sec. The relative expression levels of Bcl-2, Bax, VEGF, basic fibroblast growth factor (bFGF), angiopoietin-2 (Ang-2), and PCNA were normalized to the GAPDH internal control. The relative transcription levels of the target genes were calculated using the relative mRNA quantification, the $2^{-\Delta\Delta Ct}$ method: $\Delta\Delta CT = \Delta Ct_{(target\ gene)} - \Delta Ct_{(internal\ control)}$ [16]. Relative transcription levels of target genes = $2^{-\Delta\Delta Ct}$.

Table I. Sequences of primers.

Name	Sequence
FGF7	F: 5'-AATGATGAAGCCCTGGAGTG-3' R: 5'-TTTCTTGCGCTTTCGTTTTT-3'
Bcl-2	F: 5'-CCTTTGTGTAACTGTACGGCC-3' R: 5'-CTTTGGCAGTAAATAGCTGATTCGAC-3'
Bax	F: 5'-GTGCACCAAGGTGCCGGAAC-3' R: 5'-TCAGCCCATCTTCTTCCAGA-3'
VEGF	F: 5'-CAGCCCCAGCTACCACCTC-3' R: 5'-TCTTCCTCCTCCCCCTCCTC-3'
PCNA	F: 5'-GAGTGGTCGTTGTCTTTC-3' R: 5'-GCGGCAACAACGCCGCTA-3'
bFGF	F: 5'-CCGGAATTCTTCAAGGACCCCAAGCGGCT-3' R: 5'-CCCAAGCTTGGCCATTAAAATCAGCTCTT-3'
Ang-2	F: 5'-GGATCTGGGGAGAGAGGAAC-3' R: 5'-CTCTGCACCGAGTCATCGTA-3'
GAPDH	F: 5'-AGCCACATCGCTCAGACACC-3' R: 5'-GTACTCAGCGGCCAGCATCG-3'

FGF7: fibroblast growth factor 7; Bcl-2: B-cell lymphoma 2; Bax: Bcl-2-associated X protein; VEGF: vascular endothelial growth factor; bFGF: basic fibroblast growth factor; Ang-2: angiopoietin-2; PCNA: proliferating cell nuclear antigen.

Protein Expression of Genes by Western Blot

Cells were collected 48 hours after transfection and 1 ml of lysate was added with shaking once every 10 min. The mixtures were then centrifuged at 4°C for 20 min at a speed of 4,000 r/min. The levels of the proteins were determined by BCA Protein Assay Kit (Shanghai Yeasen Biotechnology Co. Ltd., Shanghai, China) and the samples were then stored at -20°C for subsequent use. SDS-PAGE gels of 10% were prepared with two layers, separating gel, and stacking gel. The samples were mixed with the sample buffer, and boiled at 100°C for 5 min. The samples were loaded on the gel and were transferred to polyethylene difluoride (PVDF) membranes after electrophoresis. The membranes were blocked with Tris-Buffered Saline and Tween 20 (TBST) containing 5% BSA for 1 h, and were then incubated overnight at 4°C with primary antibodies, including rabbit anti-human FGF7 antibody (1:1,000, ab131162, Abcam, Cambridge, UK), rabbit anti-human Bcl-2 antibody (1:1,000, ab32124, Abcam, Cambridge, UK), rabbit anti-human Bax antibody (1:1,000, ab32503, Abcam, Cambridge, UK), rabbit anti-human VEGF antibody (1:5,000, ab11939, Abcam, Cambridge, UK), rabbit anti-human bFGF antibody (1:1,000, ab92337, Abcam, Cambridge, UK), rabbit anti-human Ang-2 antibody (1:2,000, ab92445, Abcam, Cambridge, UK), and rabbit anti-human PCNA antibody (1:1,000, ab92552, Abcam, Cambridge, UK). After incubation, the membranes were washed with phosphate-buffered saline (PBS) for 3 times at room temperature, each time 5 min, followed by incubation with horseradish peroxidase-conjugated goat anti-rabbit IgG at 37°C for 1 h with shaking (1:1,000, Wuhan Boster Biological Technology Ltd., Wuhan, China). The membranes were then washed with PBS for 3 times at room temperature, each time 5 min, and were immersed in enhanced chemiluminescent (ECL) Western Blotting Substrate (Pierce, Rockford, Illinois, USA) at room temperature for 1 min. After removal of reagent with pipette, the membranes were wrapped with

the plastic wrap, and were processed in a dark room for exposure and imaging using X-ray film. GAPDH was used as an internal control, and the relative expression levels of the proteins were calculated as the ratio of the gray value of the target band to the gray value of internal control band using ImageJ 2.0 software.

Cell Viability by MTT Assay

Cells of all groups were collected and counted 48 h after transfection and seeded into a 24-well plate at a density of $3*10^3$ - $6*10^3$ per well, or 0.1 ml per well, five replicate wells for each group. The plate was then cultured in the incubator. The following experiment was carried out at 24 h, 48 h, and 72 h after the culture. A 20 μl of 5 mg/ml MTT solution (Wuhan Procell Life Science & Technology Co., Ltd., Wuhan, China) was added to each well and the plate was incubated at 37°C for 2 h. Then, the culture was terminated, and the supernatants were discarded, with 150 μl of dimethyl sulfoxide (DMSO) solution added to each well. The optical density (OD) measurement was performed with a microplate reader (NYW-96M, Beijing Nuoyawei Instrument Co., Ltd., Beijing, China) at 492 nm wavelength. The figure related to cell viability was plotted with the time point as the abscissa and the OD value as the ordinate.

Cell Invasion Rate by Transwell Invasion Assay

Cells were collected after 48 h of culture and washed with PBS buffer for 3 times, each time 5 min, and 0.25% trypsin (Thermo Fisher Scientific, Inc., Waltham, MA, USA) was added for the dissociation of cells. Serum-free medium was then added to the dissociated cells to prepare single cell suspension. The cells were counted, and the cell density was adjusted to $1*10^5$ cells /ml. An appropriate amount of diluted Matrigel was added to the bottom of the transwell chamber and the transwell was incubated overnight. Then, a 100 μl ($1*10^5$ cells /ml) of cell suspension was added to the upper chamber of the transwell and a 500 μl of 10% FBS to its lower chamber. The cells were incubated at 37°C in a 5% CO_2 incubator for 48 h. After incubation, non-invaded cells on the top of the transwell were scraped off. The transwell was rinsed with PBS, fixed at room temperature for 30 min with 4% paraformaldehyde, stained with 1% crystal violet, and rinsed with PBS. The transwell was dried by placing it upside down on the glass slide. Photos were taken under light microscope and the cells that passed through the membrane were counted. For each sample, invaded cell numbers were determined by calculating the average cell number of 5 fields of view. Invasion rate = (mean invaded cell number of control chamber - mean invaded cell number of sample chamber) / mean invaded cell number of control chamber * 100%.

Cell Proliferation and Apoptosis by Flow Cytometry

Cells were harvested 48 h after transfection, and were washed with PBS buffer for three times, each time 5 min. After washing, the cells were centrifuged for 20 min at 4,000 r/min. Resuspension was performed after the supernatants were discarded. The cell density was adjusted to $1*10^5$ cells /ml, and 1 mL of 75% ethanol pre-cooled at -20°C was added to fix cells for 1 h. Then, centrifugation was conducted at 2,000 r/min for 15 min, and the cells were rinsed with PBS for 2 times, each time for 3 min. The supernatants were discarded and 100 μl of RNase A (Guangzhou Geneseed Biotech Co., Ltd., Guangzhou, China) was added to cells, followed by incubation in a water bath for 30 min at 37°C. Four hundred microliter of propidium iodide (PI; Sigma-Aldrich, Inc., St. Louis, MO, USA) was used for staining in the dark at 4°C for 30 min. The cell cycle was detected by flow cytometer FACS-Calibur for fluorescence in red at an excitation wavelength of 488 nm. S-phase fraction (SPF) = S / (G0/1+S+G2/M) * 100% and proliferation index (PI) = (S + G2 / M) / (G0/1 + S + G2 / M) * 100%.

After 48 h of transfection, the cells were collected and dissociated with Ethylene Diamine Tetraacetic Acid (EDTA)-free trypsin. After dissociation, the cells were collected into tubes for flow cytometry, rinsed with cold PBS for 3 times, each time 5 min, and centrifuged at 4000 r/min for 15 min before the supernatants were discarded. Cell apoptosis was detected using Annexin V-Fluorescein Isothiocyanate (Annexin V-FITC) Apoptosis Detection Kit (Sigma-Aldrich, Inc., St. Louis, MO, USA) according to its instructions. Annexin-V-FITC/propidium iodide (PI) dye liquor was made with Annexin-V-FITC, propidium iodide, and N-2-hydroxyethylpiperazine-N-ethane-sulphonicacid (HEPES) buffer (proportion: 1:2:50); and $1*10^6$ cells were resuspended per 100 μl dye liquor and evenly oscillated. The cells were then incubated at room temperature for 15 min before being added with 1 ml of HEPES buffer and evenly oscillated. Flow cytometer FACS-Calibur was used to excite band pass filters of 520 nm

and 620 nm at a wavelength of 488 nm to detect FITC and PI fluorescence, respectively, for measuring cell apoptosis. Cell apoptosis = number of apoptotic cells / total number of cells * 100%.

Statistical Analysis

All statistical data were processed using Statistical Product Service Solution (SPSS; IBM Corp., Armonk, NY, USA) 21.0 software package. For the measurement data, the results of each parameter were expressed by the mean ± standard deviation ($\bar{x}$ ± SD). Comparison among groups was based on One-way analysis of variance. When there were significant differences among groups, Bonferroni post-hoc test was used for pairwise comparison. A p-value of <0.05 was considered statistically significant.

Results

mRNA Expression of FGF7, Bcl-2, Bax, VEGF, bFGF, Ang-2, and PCNA

The results of qRT-PCR were shown in Table II. The mRNA expressions of FGF7, Bcl-2, VEGF, bFGF, Ang-2, and PCNA were significantly increased in other groups than in the normal group, and the mRNA expression of Bax was significantly decreased in other groups than in the normal group (all $p < 0.05$). There were no significant differences in mRNA expressions of all genes between the blank group and the NC group (all $p > 0.05$). The mRNA expressions of FGF7, Bcl-2, VEGF, bFGF, Ang-2, and PCNA were significantly lower in the si-FGF7 group than in the blank group, and the mRNA expression of Bax was significantly higher in the si-FGF7 group than in the blank group (all $p < 0.05$).

Protein Expression of FGF7, Bcl-2, Bax, VEGF, bFGF, Ang-2, and PCNA

The results of Western blot were shown in Figure 1. The protein expressions of FGF7, Bcl-2, VEGF, bFGF, Ang-2, and PCNA were significantly increased in other groups than in the normal group, and the protein expression of Bax was significantly decreased in other groups than in the normal group (all $p < 0.05$). There were no significant differences in the protein expressions of all genes between the blank group and the NC group (all $p > 0.05$). The protein expressions of FGF7, Bcl-2, VEGF, bFGF, Ang-2, and PCNA were significantly lower in the si-FGF7 group than in the blank group, and the protein expression of Bax was significantly higher in the si-FGF7 group than in the blank group (all $p < 0.05$).

Comparison of Cell Viability

The results of MTT assay were shown in Figure 2. At 24 h, there was no significant difference in cell viability among four groups ($p > 0.05$). The cell viability of each group increased over time (all $p < 0.05$). At 48 h and 72 h, the cell viabilities of other groups were significantly elevated than those of the normal group (all $p < 0.05$). There was no significant difference in the change of overall cell viability between the blank group and the NC group ($p > 0.05$). At 48 h and 72 h, the cell viabilities of the si-FGF7 group were significantly lower than those of the blank group (both $p < 0.05$).

Table II. mRNA expressions of FGF7, Bcl-2, Bax, VEGF, bFGF, Ang-2, and PCNA.

Gene	Normal	Blank	NC	si-FGF7	F	p
FGF7	0.99±0.09	1.68±0.13*	1.69±0.13*	1.34±0.11*#	24.57	0.0002
Bcl-2	0.99±0.09	1.67±0.12*	1.63±0.12*	1.31±0.11*#	24.65	0.0002
Bax	1.00±0.10	0.41±0.03*	0.42±0.03*	0.78±0.07*#	59.85	<0.0001
VEGF	1.01±0.10	1.77±0.13*	1.79±0.14*	1.36±0.11*#	28.36	0.0001
bFGF	0.32±0.05	1.42±0.23*	1.39±0.18*	0.76±0.08*#	35.90	<0.0001
Ang-2	0.21±0.04	1.14±0.15*	1.11±0.12*	0.52±0.05*#	61.08	<0.0001
PCNA	0.98±0.09	1.75±0.12*	1.80±0.13*	1.41±0.13*#	30.56	<0.0001

Normal group: Human normal retinal vascular endothelial cells ACBRI-181; Blank group: Retinoblastoma cell line HXO-Rb44 without plasmid transfection; Negative Control (NC) group: Retinoblastoma cell line HXO-Rb44 with transfection of FGF7 plasmid; si-FGF7 group: Retinoblastoma cell line HXO-Rb44 with transfection of FGF7 siRNA plasmid. FGF7: fibroblast growth factor 7; Bcl-2: B-cell lymphoma 2; Bax: Bcl-2-associated X protein; VEGF: vascular endothelial growth factor; bFGF: basic fibroblast growth factor; Ang-2: angiopoietin-2; PCNA: proliferating cell nuclear antigen. Compared with the normal group, *p<0.05; compared with the blank group, #p<0.05.

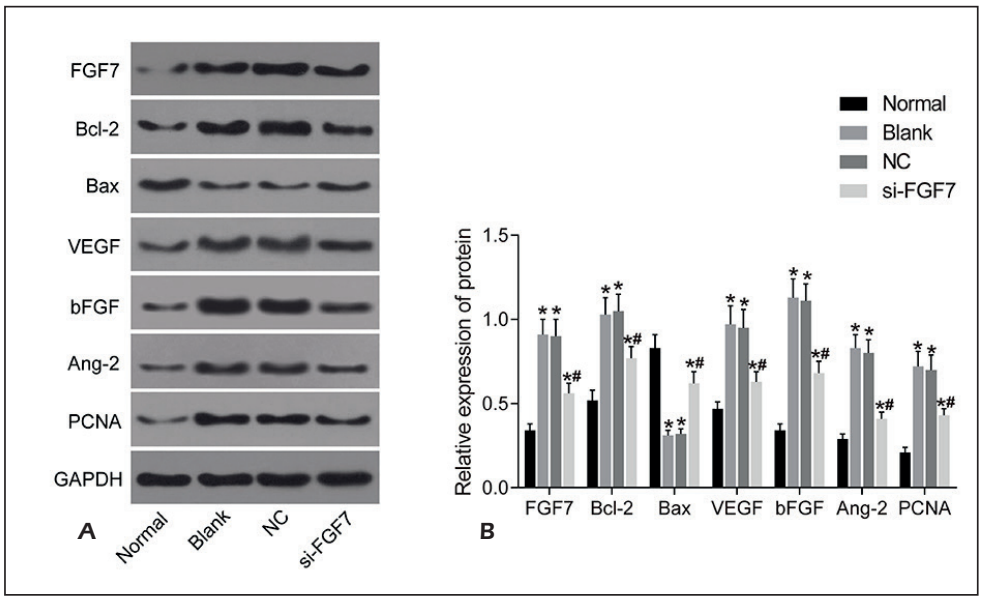

Figure 1. Protein expressions of FGF7, Bcl-2, Bax, VEGF, bFGF, Ang-2 and PCNA. **A**, Protein bands of FGF7, Bcl-2, Bax, VEGF, bFGF, Ang-2 and PCNA in each group of cells. **B**, Relative protein expression levels of FGF7, Bcl-2, Bax, VEGF, bFGF, Ang-2 and PCNA in each group of cells. Normal group: Human normal retinal vascular endothelial cells ACBRI-181; Blank group: Retinoblastoma cell line HXO-Rb44 without plasmid transfection; Negative Control (NC) group: Retinoblastoma cell line HXO-Rb44 with transfection of FGF7 plasmid; si-FGF7 group: Retinoblastoma cell line HXO-Rb44 with transfection of FGF7 siRNA plasmid. Compared with the normal group, *p<0.05; compared with the blank group, $^{\#}p$<0.05. NC: negative control; FGF7: fibroblast growth factor 7; Bcl-2: B-cell lymphoma 2; Bax: Bcl-2-associated X protein; VEGF: vascular endothelial growth factor; bFGF: basic fibroblast growth factor; Ang-2: angiopoietin-2; PCNA: proliferating cell nuclear antigen.

Comparison of Invasive Capability of Cells

The results of the transwell invasion assay were shown in Figure 3. The invasion rates of the other groups were significantly higher than that of the normal group (all $p < 0.05$). There was no significant difference in invasion rate between the blank group and the NC group ($p > 0.05$). The invasion rate of the si-FGF7 group was significantly lower than that of the blank group ($p < 0.05$).

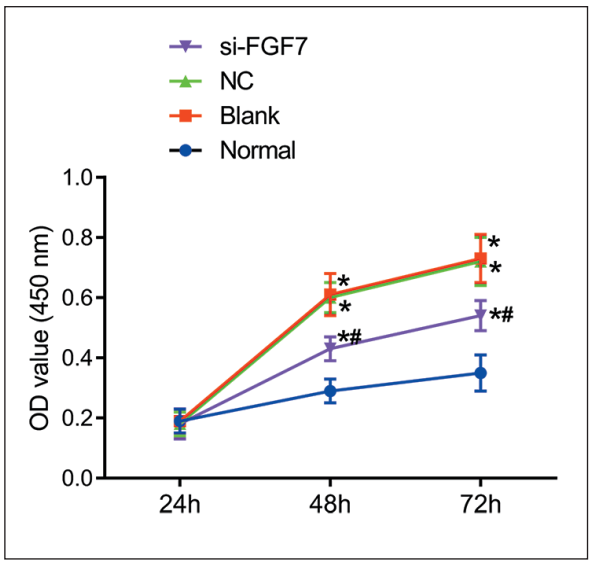

Figure 2. Cell viability. Compared with the normal group, *p<0.05; compared with the blank group, $^{\#}p$<0.05. NC: negative control; OD: optical density; FGF7: fibroblast growth factor 7.

Comparison of Cell Proliferative Capability

The results of PI staining were shown in Figure 4. The SPF in other groups was significantly increased than that in the normal group (all $p < 0.05$). There was no significant difference in SPF between the blank group and the NC group ($p > 0.05$). Compared with the blank group, the si-FGF7 group had significantly lower SPF ($p < 0.05$), indicating reduced cell proliferation in the si-FGF7 group.

Comparison of Cell Apoptosis Rate

The results of cell apoptosis assay were shown in Figure 5. The apoptosis rates of other groups were significantly lower than that of the normal group (all $p < 0.05$). There was no significant difference in apoptosis rate between the blank group and the NC group ($p > 0.05$). Compared with the blank group, the cell apoptosis rate of si-FGF7 group was significantly increased ($p < 0.05$).

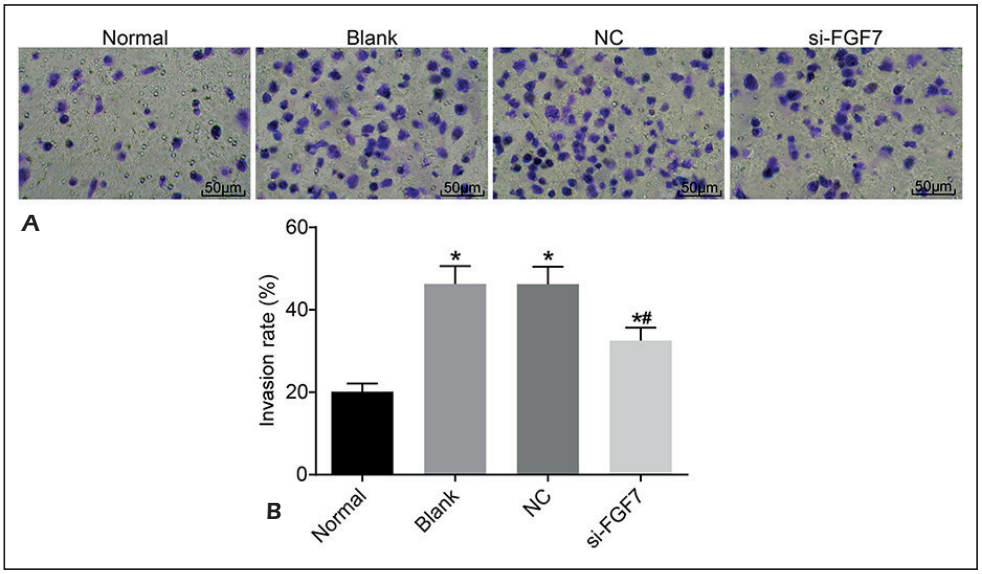

Figure 3. Cell invasion. **A**, Transwell invasion assay of cells of each group (200×). **B**, The invasion rate of each group. Compared with the normal group, *p<0.05; compared with the blank group, $^{\#}p$<0.05. NC: negative control; FGF7: fibroblast growth factor 7.

Discussion

Fibroblast growth factor (FGF) is a common peptide in the human body that possesses a wide range of biological activities[17]. By binding to its receptors, it can participate in various signal transduction pathways in cells and play an important role in the cellular immune response and the growth and development of various organs[18]. Mehta et al[19] observed by screening mutation genes in prostate cancer that FGF7 gene mutation plays an important role in the development and progression of prostate cancer. Elhefnawi et al[20] found that FGF7 gene was abnormally expressed in hepatocellular carcinoma when analyzing the differential expression of miRNAs and genes in hepatocellular carcinoma. Turczyk et al[21] found that FGF7 can promote the growth of breast can-

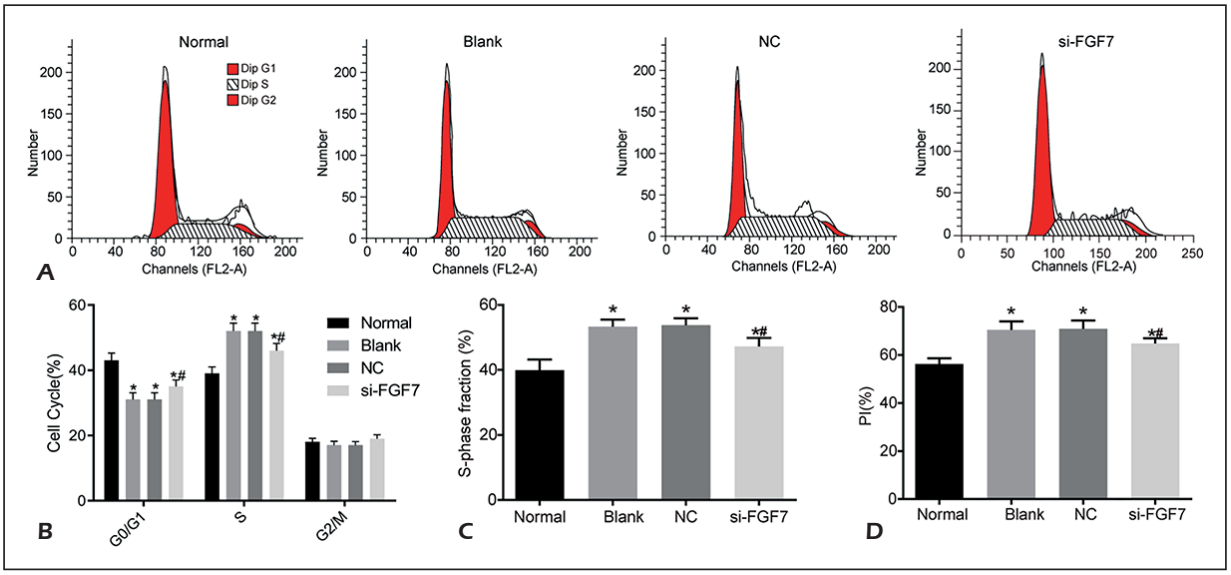

Figure 4. Comparison of cell proliferative capability. **A**, Images of cell cycle by flow cytometry 48 h after transfection. **B**, Changes in cell cycle of each group 48 h after transfection. **C**, SPF in each group 48 h after transfection. **D**, PI of each group 48 h after transfection. Compared with the normal group, *p<0.05; compared with the blank group, $^{\#}p$<0.05. NC: negative control; SPF: S-phase fraction; PI: proliferation index; FGF7: fibroblast growth factor 7.

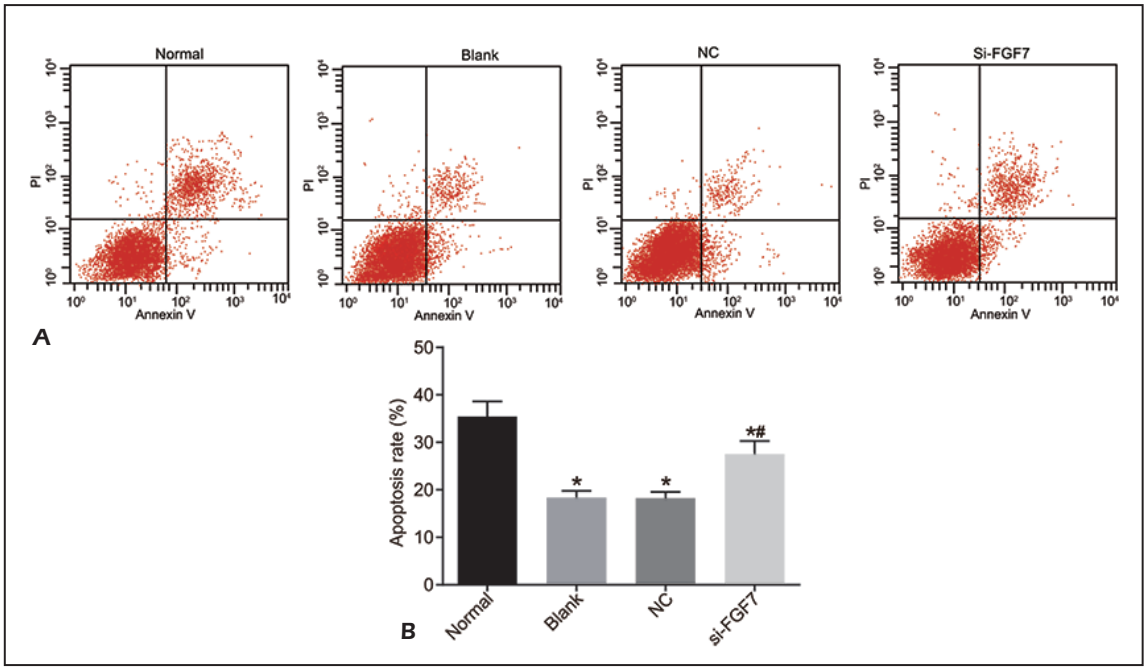

Figure 5. Cell apoptosis. **A**, Images of cell apoptosis by flow cytometry 48 h after transfection. **B**, Apoptosis rate of each group 48h after transfection. Compared with the normal group, *$p<0.05$; compared with the blank group, $^{\#}p<0.05$. NC: negative control; PI: proliferation index; FGF7: fibroblast growth factor 7.

cer cells, and its expression is also closely related to the drug resistance of breast cancer patients. These studies have confirmed the role of FGF7 in the development and progression of tumors.

Currently, malignant tumors are characterized by uncontrolled proliferation. The proliferation and apoptosis of tumor cells are regarded as important factors in the development and progression of tumors[22]. In this study, the expression of FGF7 in RB cells HXO-Rb44 was interfered by transfecting FGF7 siRNA. The results of qRT-PCR and Western blot revealed that the expression of FGF7 in other groups was significantly higher than that of the normal group before transfection, indicating that FGF7 may play a role in the progression of RB. Bcl-2 is a typical anti-apoptotic gene, and Bax, a typical pro-apoptotic gene, both of which have important correlations with cell apoptosis and survival[23]. As a common protein associated with cell cycle, PCNA can bind to DNA polymerase accessory proteins and thus participate in DNA replication. Previous studies[24,25] have detected that it is involved in the proliferation of a variety of tumor cells. In this study, the mRNA and protein expression of Bcl-2 and PCNA in RB cell lines HXO-Rb44 of all groups, except the normal group, was significantly increased, but the mRNA and protein expression of Bax was significantly decreased, indicating that the proliferation of RB cells was promoted and their apoptosis was significantly inhibited. After silencing FGF7 in RB cell line HXO-Rb44, the above conditions were significantly improved, with cell proliferation significantly suppressed, and the expression of pro-apoptotic factors elevated. Moreover, cell viability and apoptosis were detected by MTT assay and flow cytometry in this study. The comparison between the si-FGF7 group and the blank group showed that the inhibition of FGF7 expression reduced the proliferation of RB cells. Moreover, the SPF in the si-FGF7 group was decreased, and its apoptosis rate significantly increased. This validated the significance of FGF7 gene silencing in inhibiting RB cell proliferation and promoting apoptosis. As one of the biological characteristics of tumor metastasis, cell invasion mainly refers to the process in which tumor cells enter the microcirculation through lymphatic and microvascular tissues and are then transferred to the neighboring tissues[26]. In this study, transwell invasion assay was used to detect the invasive capability of the cells of each group. The results showed that the invasive capability of cells in the si-FGF7 group was significantly lower than that in the blank group, indicating the value of FGF7 gene silencing in inhibiting RB cell invasion.

Hypoxia is one of the important features of solid tumors, and tumor neovascularization can provide sufficient oxygen and nutrients for tumor

cells, which is crucial to the acceleration of tumor growth, migration, and invasion[27]. VEGF is a key factor in the process of neovascularization. It can not only promote tumor growth by accelerating tumor angiogenesis, but also accelerate the secretion of collagenases in endothelial cells by increasing vascular permeability, which can speed up the invasion and metastasis of tumor cells[28]. Li et al[29] found that the VEGF expression was significantly upregulated in human RB tissues. Song et al[30] also confirmed that the VEGF protein is highly expressed in RB cells under hypoxic conditions, and it can accelerate tumor angiogenesis by increasing vascular extracellular matrix. bFGF is widely distributed in the body, and there are many studies on its role in tumor angiogenesis; Ang-2 also plays an important part in regulating angiogenesis and synergizes with the expression of bFGF[31,32]. In this study, qRT-PCR and Western blot were used to detect the expression of VEGF. After silencing FGF7 in RB cells, the expression of VEGF, bFGF, and Ang-2 in cells was significantly decreased.

In this report, we investigated the effects of inhibited FGF7 expression on the biological characteristics of RB cells and tumor angiogenesis. However, we did not identify whether FGF7 regulates RB through downstream signaling pathways, which should be determined in future studies.

Conclusions

FGF7 gene silencing can inhibit the proliferation and invasion of RB cells and angiogenesis, accelerate cell apoptosis, and thus suppress tumor growth. The role of FGF7 in RB may be achieved by affecting the regulation of its downstream apoptosis-related and angiogenesis-related genes. FGF7 has the potential to be an important target in the treatment of RB.

Conflict of Interests

The authors declare that they have no conflict of interest.

References

1) Nassr M, Wang X, Mitra S, Freemananderson NE, Patil R, Yates CR, Miller DD, Geisert EE. Treating retinoblastoma in tissue culture and in a rat model with a novel isoquinoline derivative. Invest Ophthalmol Vis Sci 2017; 51: 3813.
2) Murali A, Varghese BT, Kumar RR, Kannan S. Combination of genetic variants in cyclin D1 and retinoblastoma genes predict clinical outcome in oral cancer patients. Tumour Biol 2016; 37: 3609-3617.
3) Ortiz MV, Dunkel IJ. Retinoblastoma. J Child Neurol 2016; 31: 227.
4) Li X, Yang L, Shuai T, Piao T, Wang R. MiR-433 inhibits retinoblastoma malignancy by suppressing Notch1 and PAX6 expression. Biomed Pharmacother 2016; 82: 247-255.
5) Liu X, Sun K, Wang H, Dai Y. Knockdown of retinoblastoma protein may sensitize glioma cells to cisplatin through inhibition of autophagy. Neurosci Lett 2016; 620: 137-142.
6) Qi DL, Cobrinik D. MDM2 but not MDM4 promotes retinoblastoma cell proliferation through p53-independent regulation of MYCN translation. Oncogene 2016; 36: 1760-1769.
7) Jia M, Wei Z, Liu P, Zhao X. Silencing of ABCG2 by microRNA-3163 inhibits multidrug resistance in retinoblastoma cancer stem cells. J Korean Med Sci 2016; 31: 836-842.
8) Lupo G, Motta C, Salmeri M, Spina-Purrello V, Alberghina M, Anfuso CD. An in vitro retinoblastoma human triple culture model of angiogenesis: a modulatory effect of TGF-β. Cancer Lett 2014; 354: 181-188.
9) Yang H, Cheng R, Liu G, Zhong Q, Li C, Cai W, Yang Z, Ma J, Yang X, Gao G. PEDF inhibits growth of retinoblastoma by anti-angiogenic activity. Cancer Sci 2010; 100: 2419-2425.
10) Rubin JS, Osada H, Finch PW, Taylor WG, Rudikoff S, Aaronson SA. Purification and characterization of a newly identified growth factor specific for epithelial cells. Proc Natl Acad Sci USA 1989; 86: 802-806.
11) Finch PW, Rubin JS, Miki T, Ron D, Aaronson SA. Human KGF is FGF-related with properties of a paracrine effector of epithelial cell growth. Science 1989; 245: 752-755.
12) Husseman J, Palacios SD, Rivkin AZ, Oehl H, Ryan AF. The role of vascular endothelial growth factors and fibroblast growth factors in angiogenesis during otitis media. Audiol Neurootol 2011; 17: 148-154.
13) Huang T, Wang L, Liu D, Li P, Xiong H, Zhuang L, Sun L, Yuan X, Qiu H. FGF7/FGFR2 signal promotes invasion and migration in human gastric cancer through upregulation of thrombospondin-1. Int J Oncol 2017; 50: 1501.
14) Fan EW, Li CC, Wu WJ, Huang CN, Li WM, Ke HL, Yeh HC, Wu TF, Liang PI, Ma LJ. FGF7 Over expression is an independent prognosticator in patients with urothelial carcinoma of the upper urinary tract and bladder. J Urol 2015; 194: 223-229.
15) Shang A, Zhou C, Bian G, Chen W, Lu W, Wang W, Li D. MiR-381-3p restrains cervical cancer progression by downregulating FGF7. J Cell Biochem 2019; 120: 778-789.
16) Ayuk SM, Abrahamse H, Houreld NN. The role of photobiomodulation on gene expression of cell adhesion molecules in diabetic wounded fibroblasts in vitro. J Photochem Photobiol B 2016; 161: 368-374.

17) Presta M, Dell'Era P, Mitola S, Moroni E, Ronca R, Rusnati M. Fibroblast growth factor/fibroblast growth factor receptor system in angiogenesis. Cytokine Growth Factor Rev 2005; 16: 159-178.
18) Turner N, Grose R. Fibroblast growth factor signalling: from development to cancer. Nat Rev Cancer 2010; 10: 116-129.
19) Mehta P, Robson CN, Neal DE, Leung HY. Fibroblast growth factor receptor-2 mutation analysis in human prostate cancer. BJU Int 2000; 86: 681-685.
20) ElHefnawi M, Soliman B, Abu-Shahba N, Amer M. An integrative meta-analysis of microRNAs in hepatocellular carcinoma. Genomics Proteomics Bioinformatics 2013; 11: 354-367.
21) Turczyk L, Kitowska K, Mieszkowska M, Mieczkowski K, Czaplinska D, Piasecka D, Kordek R, Skladanowski AC, Potemski P, Romanska HM, Sadej R. FGFR2-driven signaling counteracts tamoxifen effect on erα-positive breast cancer cells. Neoplasia 2017; 19: 791-804.
22) Elenbaas JS, Mouawad R, Henry RW, Arnosti DN, Payankaulam S. Role of Drosophila retinoblastoma protein instability element in cell growth and proliferation. Cell Cycle 2015; 14: 589-597.
23) Venkatesan N, Kanwar JR, Deepa PR, Navaneethakrishnan S, Joseph C, Krishnakumar S. Targeting HSP90/Survivin using a cell permeable structure based peptido-mimetic shepherdin in retinoblastoma. Chem Biol Interact 2016; 252: 141-149.
24) Sivagurunathan S, Arunachalam JP, Chidambaram S. PIWI-like protein, HIWI2 is aberrantly expressed in retinoblastoma cells and affects cell-cycle potentially through OTX2. Cell Mol Biol Lett 2017; 22: 17.
25) Smith SJ, Hickey RJ, Malkas LH. Validating the disruption of proliferating cell nuclear antigen interactions in the development of targeted cancer therapeutics. Cancer Biol Ther 2016; 17: 310-319.
26) Neri S, Hashimoto H, Kii H, Watanabe H, Masutomi K, Kuwata T, Date H, Tsuboi M, Goto K, Ochiai A, Ishii G. Cancer cell invasion driven by extracellular matrix remodeling is dependent on the properties of cancer-associated fibroblasts. J Cancer Res Clin Oncol 2016; 142: 437-446.
27) Benavent AF, Capobianco CS, Garona J, Cirigliano SM, Perera Y, Urtreger AJ, Perea SE, Alonso DF, Farina HG. CIGB-300, an anti-CK2 peptide, inhibits angiogenesis, tumor cell invasion and metastasis in lung cancer models. Lung Cancer 2017; 107: 14-21.
28) Li F, Huang J, Ji D, Meng Q, Wang C, Chen S, Wang X, Zhu Z, Jiang C, Shi Y, Liu S, Li C. Azithromycin effectively inhibits tumor angiogenesis by suppressing vascular endothelial growth factor receptor 2-mediated signaling pathways in lung cancer. Oncol Lett 2017; 14: 89-96.
29) Li J, Zhang Y, Wang X, Zhao R. MicroRNA-497 overexpression decreases proliferation, migration and invasion of human retinoblastoma cells via targeting vascular endothelial growth factor A. Oncol Lett 2017; 13: 5021-5027.
30) Song W, Zhao X, Xu J, Zhang H. Quercetin inhibits angiogenesis-mediated human retinoblastoma growth by targeting vascular endothelial growth factor receptor. Oncol Lett 2017; 14: 3343-3348.
31) Bhushan M, Young HS, Brenchley PE, Griffiths CE. Recent advances in cutaneous angiogenesis. Br J Dermatol 2015; 147: 418-425.
32) Etoh T, Inoue H, Tanaka S, Barnard GF, Kitano S, Mori M. Angiopoietin-2 is related to tumor angiogenesis in gastric carcinoma: possible in vivo regulation via induction of proteases. Cancer Res 2001; 61: 2145.